Sang Beom Lee
Hyun Yi Kim
Jun Soo Park
Sun Hong Kwon

ISSN 1333-1124
eISSN 1849-1391

A STUDY ON THE TWO-ROW EFFECT IN THE SLOSHING PHENOMENON

UDC 629.543:629.5.045.2:532.59

Summary

In this study, changes in fluid impact loads inside a tank were examined according to a two-row tank arrangement in an LNG-FPSO (Liquefied Natural Gas-Floating Production Storage Offloading) vessel. The motion RAO (Response Amplitude Operator) of the LNG-FPSO, coupled with the sloshing phenomenon inside the tank, was calculated by using HydroStar by Bureau Veritas. The motion simulation in the tank was conducted under filling ratios of 30%H, 60%H, and 80%H. The RAO in each condition was calculated according to the one-row and the two-row tank arrangement. The motion response spectrum using the calculated RAO and the JONSWAP (Joint North Sea Wave Analysis Project) spectrum were computed by implementing irregular motion according to each filling ratio and tank arrangement. The sloshing phenomenon inside the tank was implemented by using a 6-DOF (Degree Of Freedom) sloshing motion platform; impact pressure on the walls of the tank was measured with pressure sensors installed inside the tank. The sloshing experiment was conducted under the three filling ratios in the one-row and the two-row tank arrangement and impact loads were compared under each filling ratio according to the one-row and the two-row tank arrangement.

Key words: *Sloshing phenomenon, LNG-FPSO (Liquefied Natural Gas-Floating Production Storage Offloading), CCS (Cargo Containment System), RAO (Response Amplitude Operator), Model-based testing, 6-DOF SMP (Sloshing Motion Platform), Impact load, Two-row effect, Coupling effect*

1. Introduction

The increasing demand for chemical fuels has accelerated the depletion of fossil energy sources and has enhanced negative environmental impacts such as the greenhouse effect and pollution. To resolve this problem, non-polluting energy sources have been highlighted as alternative energy for the future; related developments and commercialization have progressed in many nations. Among these sources, LNG holds an important place as it contains few harmful substances; thus, much attention has been paid to the use of LNG in terms of environmental conservation and its higher usage over the world. Owing to the increasing demand for LNG, the construction of cargo ships using LNG has increased significantly and the sizes of tanks have increased considerably. In recent years, the demand for hybrid energy ships such as LNG-FPSO has also boosted.

Vessels and floating offshore structures storing liquid cargos experience large local impact loads on the walls inside tanks owing to the fluid sloshing phenomenon, which may damage the structures. In particular, the safety of a CCS (Cargo Containment System) for an LNG is the most important design factor: the CCS must verify the safety with respect the impact load from sloshing. In addition, existing LNG cargo ships rarely operate under the partial filling condition because their primary purpose is cargo transportation, whereas LNG-FPSO vessels may experience a wide range of filling conditions because their operations such as processing, liquefaction, storage, and unloading are conducted offshore. Thus, it is essential to study the sloshing impact load in a variety of filling conditions for designing the tank of an LNG-FPSO.

Motions of vessels and floating offshore structures are severely affected by external environmental loads such as waves and wind. However, not only these external loads but also sloshing loads, i.e., sloshing phenomena inside tanks, can significantly affect the motion of floating structures that store liquid cargo. This means that the motion of floating structures is caused by the external environmental load, followed by the sloshing phenomenon from liquid cargos acting as a fluid impact load on the inside walls in tanks, thereby creating a coupling effect on the motion of floating structures. Therefore, the sloshing coupling effect must be considered for computing the motion of floating structures storing liquid cargos. Most studies examining the sloshing and the motion of floating structures have been conducted by using experimental or mathematical methods [1, 2, 3, and 4]. Malenica et al. [5] and Zalar et al. [6] conducted a numerical analysis of the coupling effect of sloshing and vessel motion by waves, whereas Rognebakke and Faltinsen [7] compared computed values with the results of sloshing coupling experiments using a two-dimensional tank model. Moirod et al. [8] computed the coupled motion of vessels using a commercial code (HydroStar) and verified the results via experiments under partial filling. Nam et al. [9, 10] calculated forces and moments caused by the sloshing phenomenon by applying a finite-difference method and the IRF (Impulse Response Function) approach and compared them with the RAO and numerical calculation results of vessel motions determined through water tank experiments.

In this study, changes in fluid impact loads inside a tank were studied according to a two-row tank arrangement in an LNG-FPSO vessel. Because the target of this study was a tank used in an LNG-FPSO, this study was conducted under a wide range of filling ratios (30%H, 60%H, and 80%H) to determine the sloshing impact load under various filling conditions. The motion RAO of the LNG-FPSO, coupled with the sloshing phenomenon inside the tank, was calculated using HydroStar by BV (Bureau Veritas). The motion response spectrum, using the calculated RAO and the JONSWAP spectrum, was computed by implementing irregular motion according to each filling ratio and tank arrangement. The sloshing phenomenon inside the modelled tank was implemented by using a 6-DOF (Degree Of Freedom) sloshing motion platform; impact pressure on the wall sides of the tank was measured by pressure sensors installed inside the tank. The sloshing experiment was conducted under the three filling ratios according to the one-row and the two-row tank arrangement; impact loads under each filling ratio according to the one-row and the two-row arrangement were compared to determine the changes in impact loads under the two-row tank arrangement.

2. Motion simulation

HydroStar, a motion analysis program by BV, was used to calculate the coupled motion RAO of the LNG-FPSO caused by the sloshing phenomenon inside the tank. HydroStar is a three-dimensional panel program [11] that analyzes the interaction between waves and floating structures by using the three-dimensional diffraction and the radiation potential theory.

2.1 Simulation Model and Conditions

In the numerical analysis, only the tanks number 2 and 4 were considered during the simulation. The reason for the selection of these tanks can be explained as follows. The tank No. 1 is smaller than any other tank. Therefore, it is usual not to analyze the sloshing load for that tank. When is comes to the tank No. 3, it is close to the center of gravity. Due to this location, the fluid motion in the tank is considered to be small. The lengths from the stern and the centers of the tanks were 237 m and 75 m, respectively. Fig. 1 shows one-row and two-row tanks with a filling ratio of 30%H and meshes of the FPSO used in the simulation. Normally, the sloshing load peaks when the incident wave is 90°. Accordingly, our motion simulation was conducted by changing the filling ratios to 30%H, 60%H, and 80%H in the tanks Nos. 2 and 4 with 100 wave frequencies of 0.18–3.142 rad/sec; the encounter angle of the incident wave was set to 90°.

Table 1 Dimensions and Loading Conditions of LNG-FPSO

L_{PP}	350.00 m
Breadth	60.00 m
Draft	12.00 m
Displacement	247,365 m^3
LCG (From A.P.)	173.733 m
VCG (From B.L.)	17.716 m
GM	14.50 m
Roll Radius of Gyration	27.00 m
Pitch Radius of Gyration	87.50 m
Yaw Radius of Gyration	87.50 m

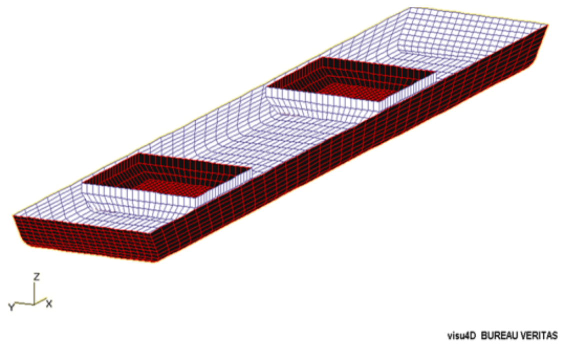

(a) One Row

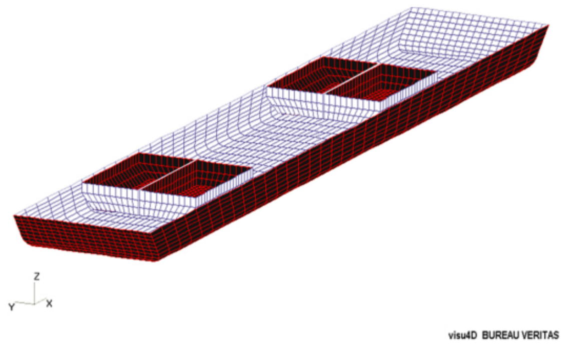

(b) Two Row

Fig. 1 Numerical Mesh of One Row and Two Row; Filling ratio: 30%H

2.2 Simulation Results

The sway and roll motion RAOs according to each filling ratio are shown in Fig. 2. As shown in the figures, when it comes to the sway, the one row motion showed more clearly resonated peaks than those of two rows. As the filling ratio increases, the peaks shown in two row results die out while the peaks in the one row remain. For a roll motion, one row shows the characteristic coupling effect of two peaks. However, two row results do not show these two peaks even though the magnitudes of the two row peaks are larger. As the filing ratio increases, the coupling effect decreases. Accordingly, the roll motion in the two-row arrangement was consistently larger than that in the one-row arrangement. The value of damping coefficient used for this simulation was 8% of the critical damping for the inside of the tank.

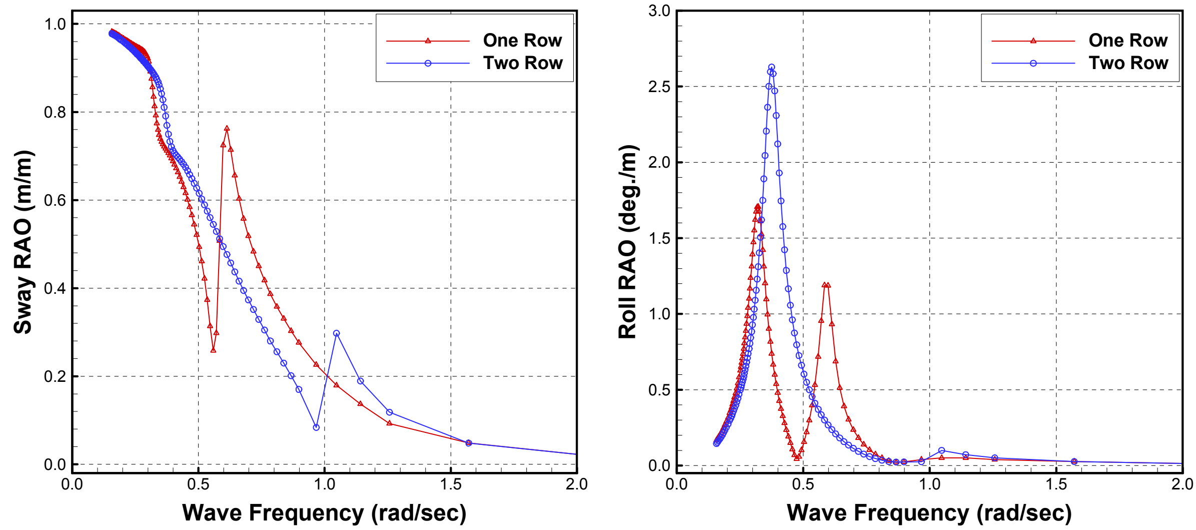

(a) Sway and Roll RAOs; Filling ratio: 30%H, Beam Sea Condition

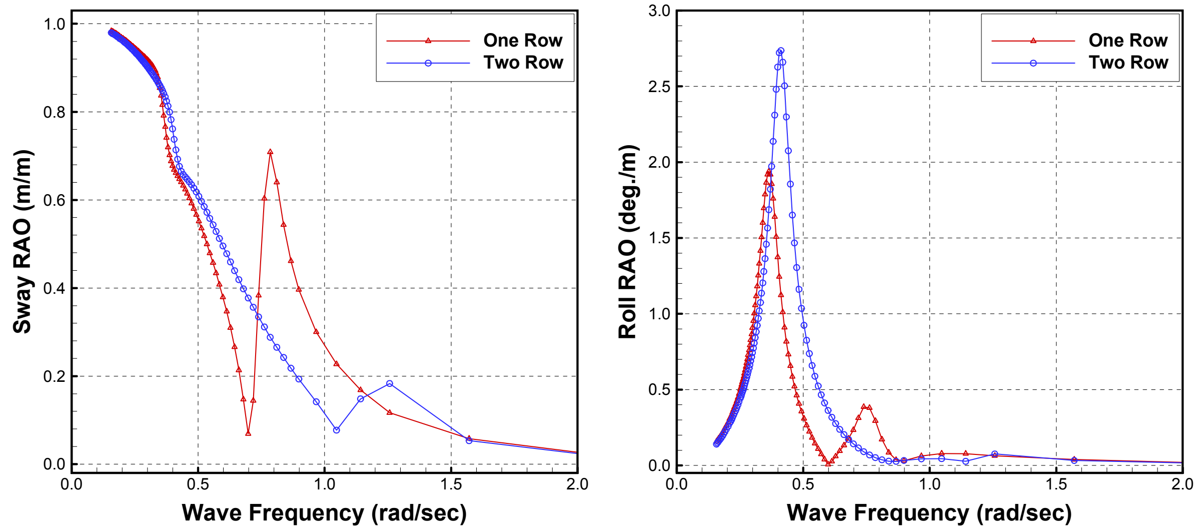

(b) Sway and Roll RAOs; Filling ratio: 60%H, Beam Sea Condition

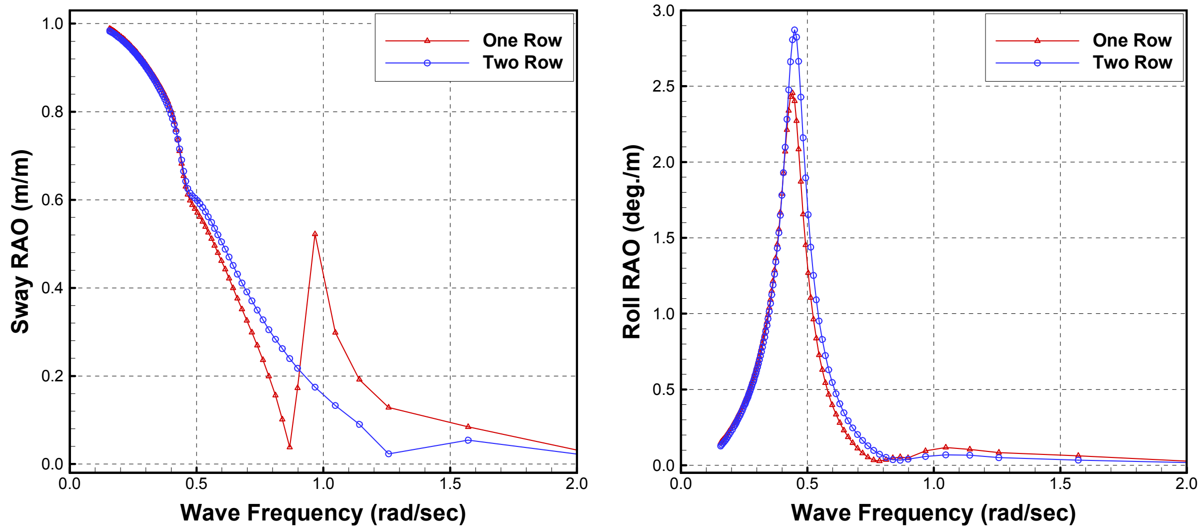

(c) Sway and Roll RAOs; Filling ratio: 80%H, Beam Sea Condition

Fig. 2 Sway and Roll RAOs; Beam Sea Condition

3. Ship motion analysis

3.1 Wave Spectrum and Conditions

To implement the irregular motion of an LNG-FPSO, the JONSWAP spectrum was used [12]. The JONSWAP spectrum is expressed by Eq. 1.

$$S(f) = \beta_J \left(H_{1/3}\right)^2 \frac{f_P{}^4}{f^5} \exp\left[-\frac{5}{4}\left(\frac{f_P}{f}\right)^4\right]\gamma^{\alpha} \tag{1}$$

where

$$\beta_J = \frac{0.0624}{0.230 + 0.0336\gamma - 0.185\left(1.9+\gamma\right)^{-1}}\left(1.094 - 0.1915\ln\gamma\right) \tag{2}$$

$$\alpha = \exp\left[-\frac{1}{2\sigma^2}\left(\frac{f}{f_P} - 1\right)^2\right] \tag{3}$$

$$f_P = \frac{1}{T_P} \tag{4}$$

$$T_P = \left(1.49 - 0.102\gamma + 0.0142\gamma^2 - 0.00079\gamma^3\right)T_Z \tag{5}$$

$$\sigma = \begin{cases} 0.07 & for \quad f \le f_P \\ 0.09 & for \quad f > f_P \end{cases} \tag{6}$$

where $H_{1/3}$ represents the significant wave height while T_Z represents the zero-crossing wave period. In addition, γ is the peak shape factor, which generally has a value from 1 to 7. In this study, a mean value of 3.3 was used.

3.2 Motion Generation

A method of reproducing the irregular motion of general floating structures in the frequency range was to calculate the motion response spectrum of a floating structure through the calculation of the wave spectrum and motion RAO, as shown in Eq. 7, by implementing a time series using the IFFT (Inverse Fast Fourier Transform).

$$S_R(\omega) = \left|H(\omega)\right|^2 \cdot S_W(\omega) \tag{7}$$

In this study, a time series of the motion for three hours, which corresponded to an actual shipping time, was calculated according to each filling ratio using Eq. 7, thereby transforming this to the No. 2 tank motion using the Euler angle method. Table 2 shows $H_{1/3}$ and T_Z per filling used in the irregular motion calculation.

To determine changes in the sway and roll motions according to the one-row and two-row arrangements, Probability Density Functions (PDF) for each motion peak value are shown in Fig. 3. As shown in the figures, both the sway and roll motions had larger mean values of the motion peaks and a wider peak distribution in the two-row arrangement than in the one-row arrangement. These results indicated that the coupling effect attributable to the sloshing phenomenon had a less marked effect on the motion in the two-row arrangement than in the one-row arrangement, as with the motion RAO.

Table 2 Wave Conditions According to Filling Ratio

Filling Ratio	Significant Wave Height ($H_{1/3}$)	Zero-Crossing Wave Period (T_Z)
30%H	9.0 m	9.5 sec
60%H	10.0 m	7.5 sec
80%H	10.0 m	7.5 sec

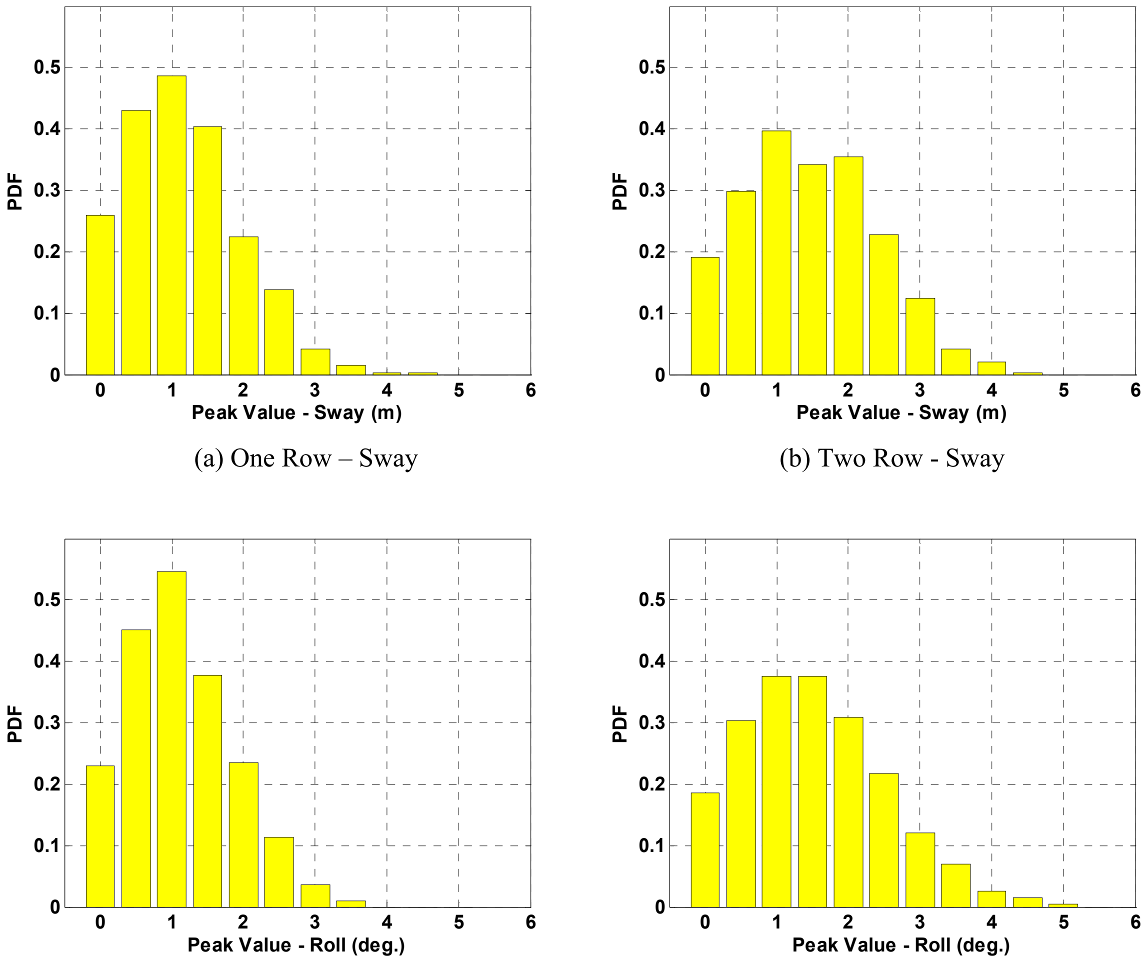

(a) One Row – Sway (b) Two Row - Sway

(a) One Row – Roll (b) Two Row - Roll

Fig. 3 Motion Peak Value Distribution in the tank No. 2; Filling ratio: 30%H

4. Experiment

4.1 Tank Model

The model experiment was conducted by using the No. 2 tank model, which was scaled to 1/50. The reduced scale model was made of 40-mm-thick acrylic to visualize the behavior of the inner fluid, and pressure sensors were attached to the inner walls of the tank by using a cluster made of brass. In addition, an attachable partition wall that divides the tank model into two halves in the longitudinal direction was installed, thereby producing an environment in which the tank model was used to determine changes in impact loads under the one-row and two-row arrangements. Fig. 4 shows the attachable partition wall in the tank model.

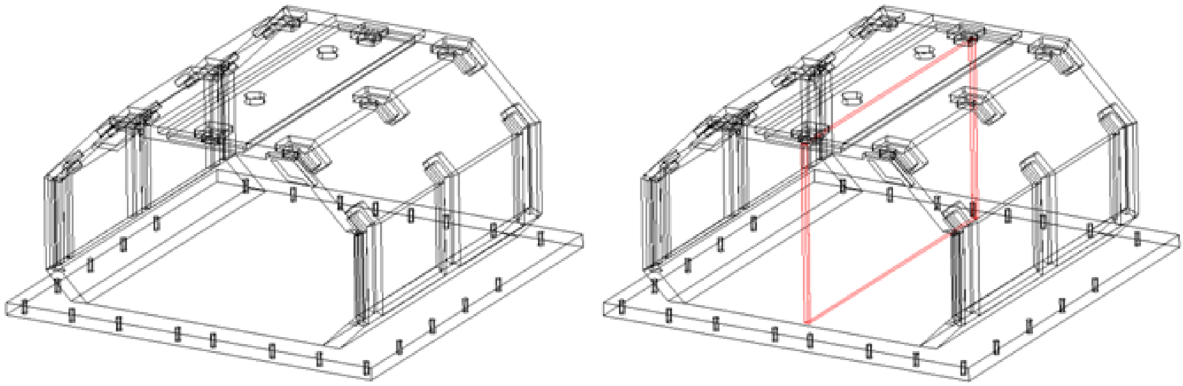

(a) One-Row Tank Model (b) Two-Row Tank Model

Fig. 4 Schematic and Image of the Tank Model

4.2 Pressure Sensor Locations

Ninety-two sensors in total were installed at places where critical impact loads were expected, to identify changes in the sloshing impact loads with the one-row and two-row tanks. The overall distribution of the pressure sensors over the tank model is shown in Fig. 5. Thirty-six sensors were installed symmetrically at the bow (#1–36) and stern (#57–92) of the tank; additional 20 sensors were installed at the front (#37–56) of the tank bow. In particular, sensors #29–36 and #85–92 were installed at places where critical impact loads were expected, owing to the presence of the partition wall. The measurement of the impact load was simplified through changes in the filling ratio by distributing the pressure sensors evenly over the tank model.

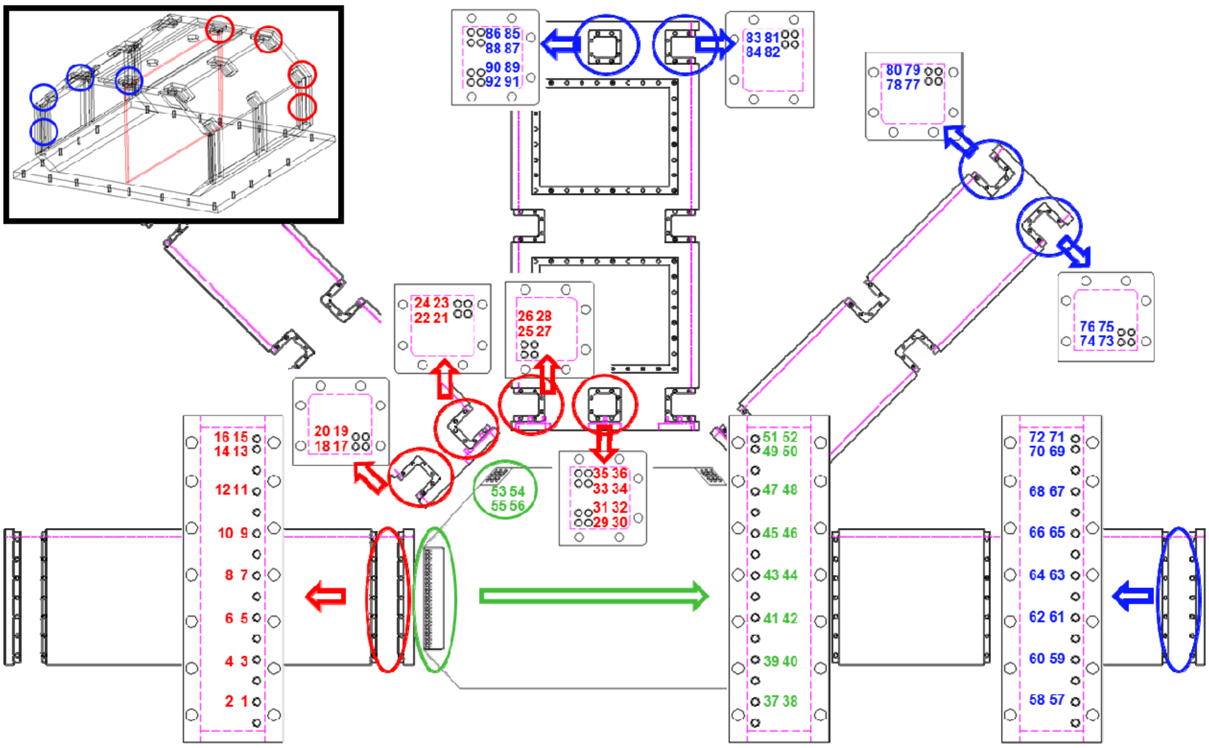

Fig. 5 Locations of Pressure Sensors

5. Results and analysis

The maximum peak pressure, the number of peak pressures, and the most probable 3-hour maximum pressure [13, 14] at each filling ratio are shown in Figs. 6-8 for the one-row and two-row arrangements. The two-row tank arrangement in all filling ratios had significantly smaller values of the maximum peak pressure and P_{3hr} than the one-row arrangement; additionally, the number of peak pressures was significantly reduced. This result reveals that the two-row arrangement reduced the sloshing phenomenon more than the one-row arrangement. Because of the reduced sloshing phenomenon, flows inside the tank were relatively stabilized, thereby reducing the number of impacts and the overall flow impact load on the walls inside the tank. However, the maximum peak pressure and P_{3hr} as well as the number of impacts measured at the #29-36 and #85-92 pressure sensors increased considerably in all filling ratios under the two-row arrangement. This happened because the above pressure sensors were located on the flat section in the one-row arrangement, whereas the locations were changed to the corner section in the two-row arrangement owing to the installation of the partition wall in the longitudinal direction. With the two-row arrangement, the phenomenon of uplifting of the inner flow along the partition wall in the tank was observed. The flow lifted along the partition wall and exerted impact on the #29–36 and #85–92 pressure sensors. In particular, this exerted a relatively large impact load in the case of 30%H with the two-row arrangement although the frequency of the impact was low (refer to Fig. 6-d).

To identify the changes in the quantitative impact load attributable to the one-row and two-row arrangements of the tank, the maximum peak pressure (P_{Max}), the top 1/10 peak pressure mean ($P_{1/10}$), the top 1/3 peak pressure mean ($P_{1/3}$), the number of peak pressures ($\#\ Peak$), and the most probable 3-h maximum pressure (P_{3hr}) measured at the sensors at each filling ratio were summarized in Table 3. Because the flow lifted along the partition wall at a filling ratio of 30%H, Sensors #92 and #90 had large values of $P_{1/10}$ and $P_{1/3}$, whereas very small numbers of total peaks were measured (#92: 14 peaks; #90: 10 peaks). In summary, the two-row arrangement at all filling ratios had lower values for most items than the one-row arrangement, as shown in Table 3. In particular, the most probable 3-hour maximum pressure with the two-row arrangement showed a more than 50% decrease in all filling ratios compared to the one-row arrangement, as well as a more than 30% decrease in the impact load occurrence frequency.

It was also verified that the two-row arrangement of the tank increased the motion (tank motion) in a relative manner, but the sloshing phenomenon inside the tank was reduced considerably, and there was a sharp decrease in the impact load exerted on the tank. However, with the two-row arrangement, a new impact load occurred in the corner section where the tank was partitioned. Therefore, it is necessary to install upper and lower chamfers in the partitioned area to reduce the impact load exerted on the corner section.

In this study, changes in fluid impact loads on the tank attributable to the decrease in the coupling effect between motions of a floating structure and the sloshing phenomenon were studied according to the two-row arrangement of a tank in an LNG-FPSO vessel.

The motion RAO of an LNG-FPSO, coupled with the sloshing phenomenon inside a tank, was calculated by using HydroStar by BV. The motion simulation was conducted in a tank under filling ratios of 30%H, 60%H, and 80%H, and the RAO in each condition was calculated according to the one-row and two-row arrangements. The motion response spectrum using the calculated RAO and the JONSWAP spectrum was computed by implementing irregular motions according to each filling ratio and tank arrangement.

The sloshing phenomenon inside the tank was implemented by using a 6-DOF sloshing motion platform; impact pressure on the walls of the tank was measured by pressure sensors installed inside the tank. The sloshing experiment was conducted under the three filling ratios according to the one-row and two-row arrangements and impact loads were compared under each filling ratio for the one-row and two-row arrangements.

Table 3 Comparison of Impact Pressures of One Row and Two Row According to the Filling Ratio

Filling Ratio	Item	One Row		Two Row		Remark
		Pressure /bar	No. Sensor	Pressure /bar	No. Sensor	
30%H	P_{Max}	1.5651	63	0.5071	42	67.6%
	$P_{1/10}$	0.2117	73	0.3690	92	-74.3%
	$P_{1/3}$	0.1411	73	0.2898	90	-105.3%
	# Peak	645	73	247	67	61.7%
	P_{3hr}	0.7579	63	0.2122	17	72.0%
60%H	P_{Max}	1.0166	82	0.8609	76	15.3%
	$P_{1/10}$	0.2330	26	0.2127	76	8.7%
	$P_{1/3}$	0.1468	25	0.1455	25	0.9%
	# Peak	592	25	223	77	62.3%
	P_{3hr}	0.6568	82	0.2594	25	60.5%
80%H	P_{Max}	1.0314	26	0.5607	28	45.6%
	$P_{1/10}$	0.2664	25	0.1683	77	36.8%
	$P_{1/3}$	0.1580	25	0.1471	77	7.0%
	# Peak	523	25	342	55	34.6%
	P_{3hr}	0.6832	25	0.3121	26	54.3%

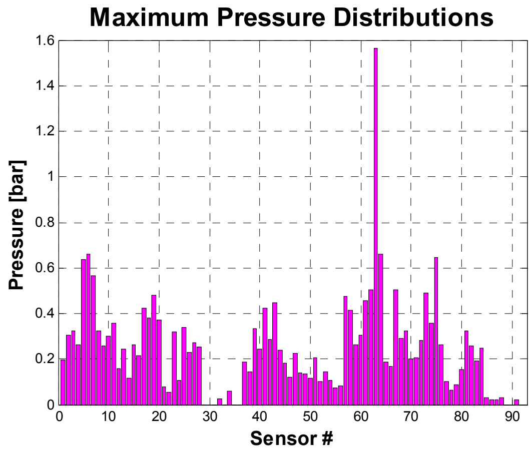

(a) One Row - Maximum Peak Pressure

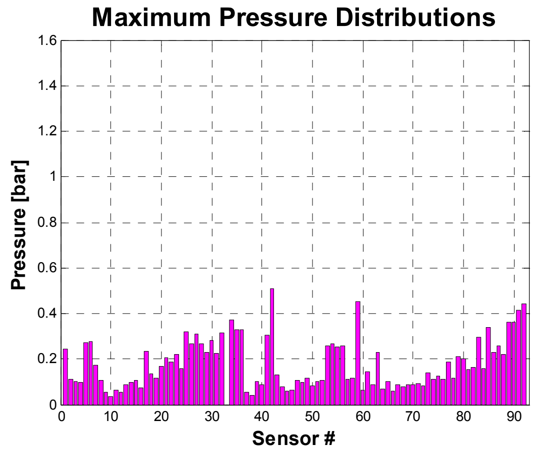

(b) Two Row - Maximum Peak Pressure

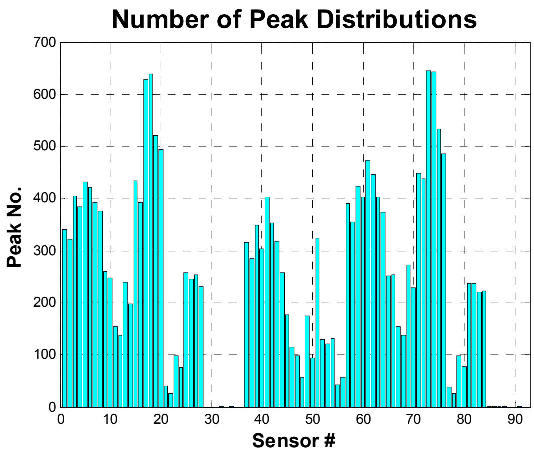

(c) One Row - Number of Peak Pressures

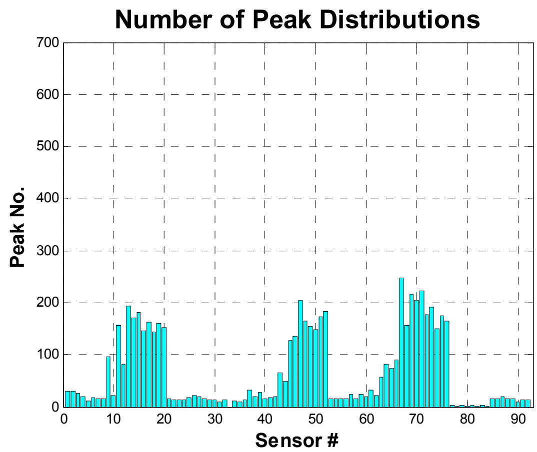

(d) Two Row - Number of Peak Pressures

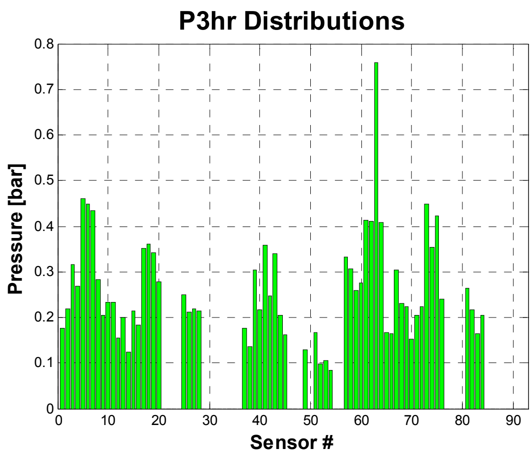

(e) One Row - P_{3hr}

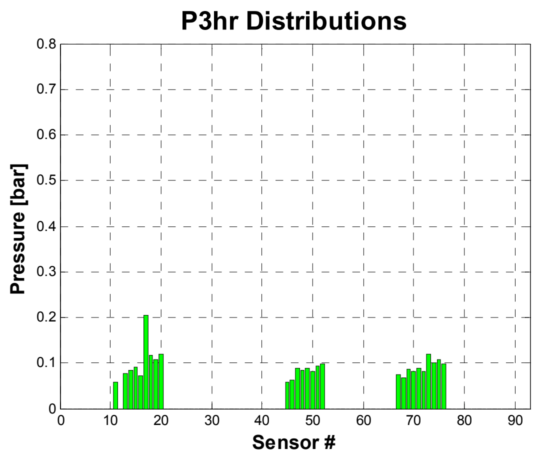

(f) Two Row - P_{3hr}

Fig. 6 Maximum Peak Pressure, Number of Peak Pressures,
and Most Probable 3-hour Maximum Pressure; Filling ratio: 30%H

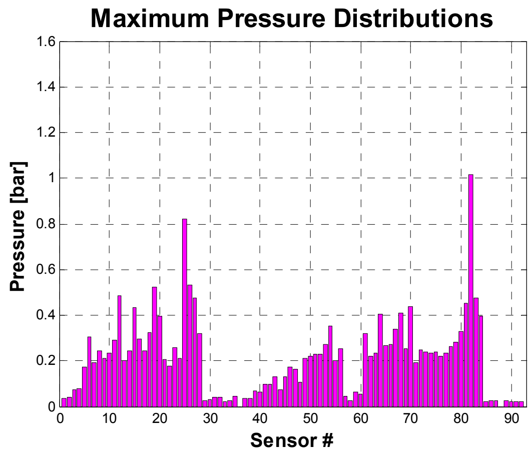

(a) One Row - Maximum Peak Pressure

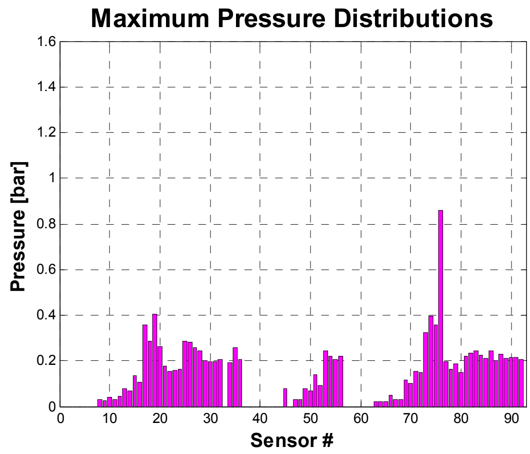

(b) Two Row - Maximum Peak Pressure

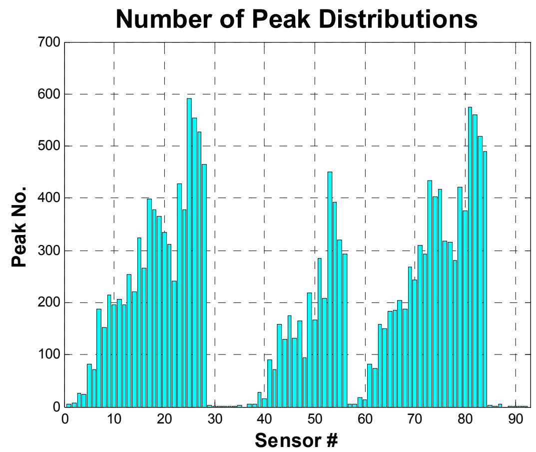

(c) One Row - Number of Peak Pressures

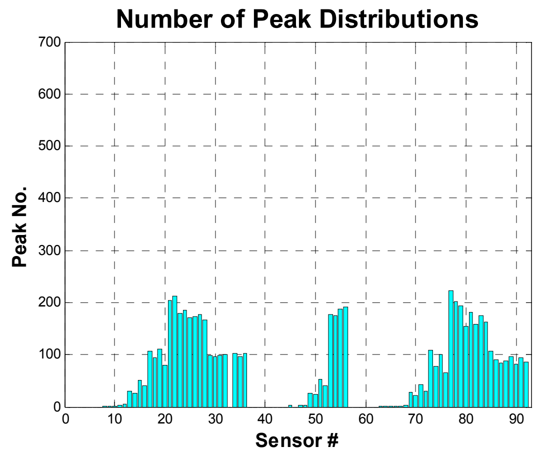

(d) Two Row - Number of Peak Pressures

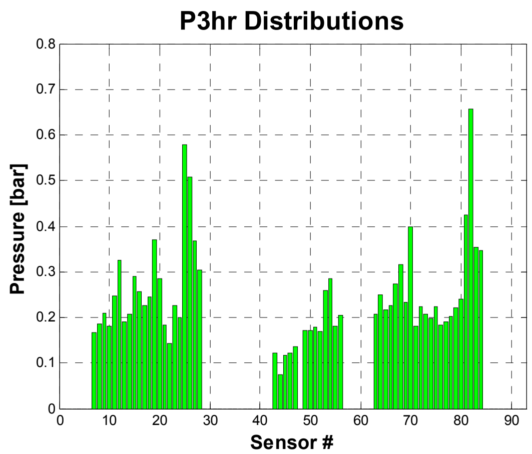

(e) One Row - P_{3hr}

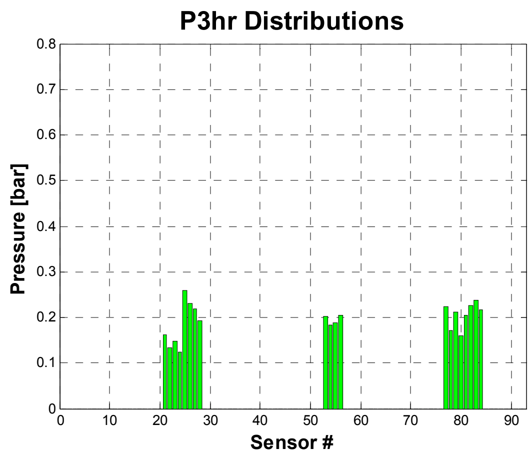

(f) Two Row - P_{3hr}

Fig. 7 Maximum Peak Pressure, Number of Peak Pressures,
and Most Probable 3-hour Maximum Pressure; Filling ratio: 60%H

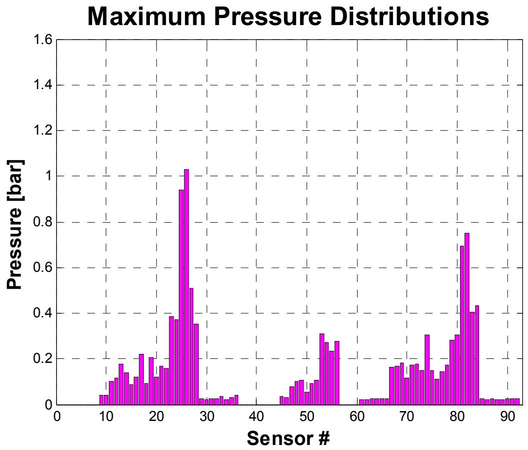

(a) One Row - Maximum Peak Pressure

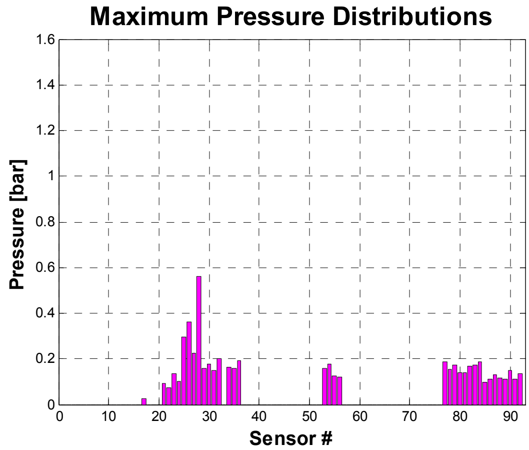

(b) Two Row - Maximum Peak Pressure

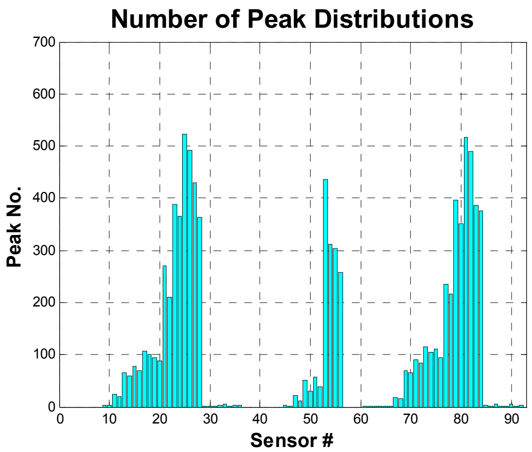

(c) One Row - Number of Peak Pressures

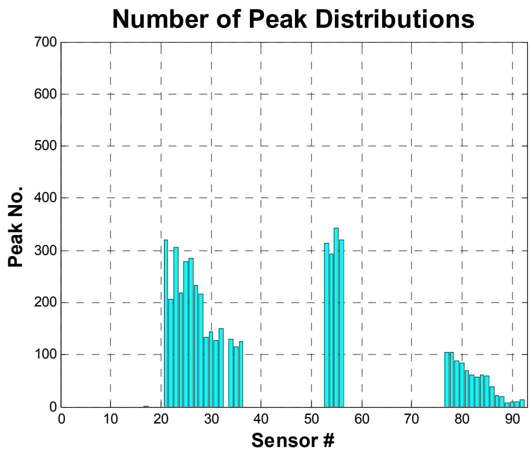

(d) Two Row - Number of Peak Pressures

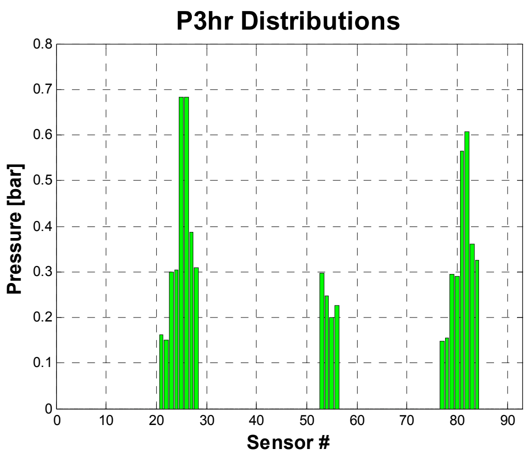

(e) One Row - P_{3hr}

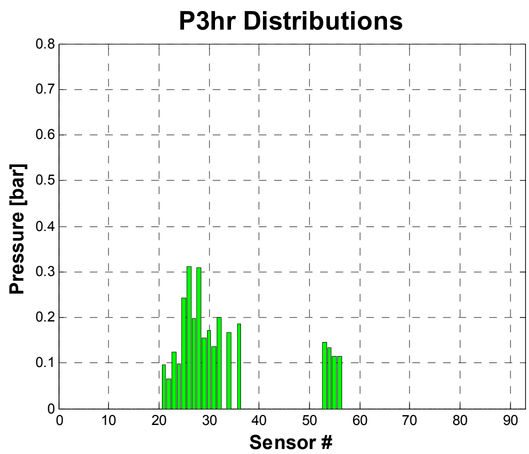

(f) Two Row - P_{3hr}

Fig. 8 Maximum Peak Pressure, Number of Peak Pressures,
and Most Probable 3-hour Maximum Pressure; Filling ratio: 80%H

6. Conclusion

In this study, changes in fluid impact loads on a tank attributable to a decrease in the coupling effect between motions of a floating structure and the sloshing phenomenon were studied according to the two-row arrangement of a tank in an LNG-FPSO vessel.

The motion RAO of an LNG-FPSO, coupled with the sloshing phenomenon inside the tank, was calculated by using HydroStar by BV. The motion simulation was conducted in the tank under filling ratios of 30%H, 60%H, and 80%H, and the RAO in each condition was calculated according to the one-row and two-row arrangements. The motion response spectrum using the calculated RAO and the JONSWAP spectrum was computed by implementing irregular motions according to each filling ratio and tank arrangement.

The sloshing phenomenon inside the tank was implemented by using a 6-DOF sloshing motion platform; the impact pressure on the walls of the tank was measured by pressure sensors installed inside the tank. The sloshing experiment was conducted under the three filling ratios according to the one-row and two-row arrangements and impact loads were compared under each filling ratio for the one-row and two-row arrangements.

At all filling ratios, the two-row arrangement showed a greater decrease in the maximum peak pressure and in the most probable 3-hour maximum pressure overall than the one-row arrangement as well as a significant number of peak pressures. This occurred because the two-row arrangement had relatively larger motion than the one-row arrangement, but the sloshing phenomenon decreased owing to the smaller size of the inside of the tank. Therefore, the two-row arrangement is more effective in ensuring the safety of the LNG CCS for vessels that hold large tanks, such as LNG-FPSO vessels.

Acknowledgment

This study was supported by the National Research Foundation of Korea (NRF) grant funded by the Korea government (MSIP) through GCRC-SOP (No. 2011-0030013).

REFERENCES

[1] Diebold, L., Baudin, E., Henry, J., Zalar, M.: Effects on Sloshing Pressure dsue to the Coupling between Seakeeping and Tank Liquid Motion, International Workshop on Water Waves and Floating Bodies, Jeju, Korea, 2008.

[2] Huang, Z.J., Danaczko, M.A., Esenkov, O.E., Martin, B.J., O'Donnell, B.J., Yung, T.W.: Coupled Tank Sloshing and LNG Carrier Motions, International Offshore and Polar Engineering Conference, Osaka, Japan, 2009.

[3] Lee, Y.B., Godderidge, B. Tan, M, Temarel, P., Turnock, S., Cowlan, N.: Coupling between Ship Motion and Sloshing Using Potential Flow Analysis and Rapod Sloshing Model, International Offshore and Polar Engineering Conference, Osaka, Japan, 2009.

[4] Mitra, S., Luong, V.H., Boo, C.K.: A Study on Complicated Coupling Effects of 3-D Sloshing in Rectangular Tanks and Ship Motion, International Offshore and Polar Engineering Conference, Osaka, Japan, 2009.

[5] Malenica, S., Zalar, M., Chen, X.B: Dynamic coupling of seakeeping and sloshing, International Offshore and Polar Engineering Conference, Honolulu, USA, 2003, pp.486~492.

[6] Zalar, M., Diebold, L., Baudin, E., Henry, J.: Sloshing Effects Accounting for Dynamics Coupling between Vessel and Tank Liquid Motion, 26th OMAE Conference, San Diego, USA, 2007.

[7] Rognebakke, O.F., Faltinsen, O.M.: Coupling of sloshing and ship motion, Journal of Ship Research 47, 2003.

[8] Moirod, N., Baudin, E., Henry, J., Diebold, L., Zalar, M.: Application of the Seakeeping/Sloshing Coupling for the LNG Terminals, International Offshore and Polar Engineering Conference, Osaka, Japan, 2009.

[9] Nam, B.W., Kim, Y., Kim, D.W., Lee, Y.B., Lee, J.H.: Study on Coupling Effects of Ship Motion and Sloshing, Proceedings of the Annual Autumn Meeting, SNAK, Yongin, Korea, 2005, pp.851~856.

[10] Nam, B.W., Yoo, D.Y., Kim, Y., Kim, D.W., Kim, Y.S.: A Study on Coupling Effects of Ship Motion and Sloshing on LNG-FPSO in Waves, Proceedings of the Annual Autumn Meeting, SNAK, Changwon, Korea, 2006, pp.666~672.

[11] Chen, X.B.: Hydrodynamics in Offshore and Naval Applications-Part Ⅰ, Keynote lecture at the 6th Intl Conference on Hydrodynamics, Perth, Australia, 2002

[12] Goda, Y.: A Comparative Review on the Functional Forms of Directional Wave Spectrum, Coastal Engineering Journal, Vol. 41, No. 1, 1999, pp. 1~20.

[13] Jung, D.W., Jung, J.H., Kwon, S.H., Park, J.S.: Stochastic Approach to Sloshing Phenomenon, Proceedings of the Annual Autumn Meeting, SNAK, Jeju, Korea, 2007, pp.1560~1569.

[14] Qiao, H., Tsokos, C.P.: Parameter estimation of the Weibull probability distribution, Mathematics and Computers in Simulation, Vol. 37, 1994, pp. 47~55.

Submitted: 28.4.2014

Accepted: 10.12.2014

Sang Beom Lee
lsb7766@pusan.ac.kr
Pusan National University
Global Core Research Center for Ships and Offshore Plants
Busan, Republic of Korea

Hyun Yi Kim
hykim01@DSME.co.kr
Daewoo Shipbuilding & Marine Engineering Co., Ltd
Hydrodynamics R&D Group
Seoul, Republic of Korea

Jun Soo Park
junsoopark@kyungnam.ac.kr
Kyungnam University
Dpt. Naval Architecture, Ocean and IT Engineering
Changwon, Republic of Korea

Sun Hong Kwon
shkwon@pusan.ac.kr*
Pusan National University
Dpt. Naval Architecture and Ocean Engineering
Busan, Republic of Korea